SI Appendix

Title:

The Mediator subunit MED31 is required for radial patterning of Arabidopsis roots

Authors:

Xiaoyue Zhang[a,b,1], Wenkun Zhou[a,d,1,2], Qian Chen[c,1,2], Mingming Fang[a,b], Shuangshuang Zheng[c], Ben Scheres[d], and Chuanyou Li[a,b,2]

Author Affiliations:

[a]State Key Laboratory of Plant Genomics and National Center for Plant Gene Research (Beijing), Institute of Genetics and Developmental Biology, Chinese Academy of Sciences, Beijing 100101, China.

[b]University of Chinese Academy of Sciences, Beijing, 100049, China.

[c]State Key Laboratory of Crop Biology, College of Agronomy, Shandong Agricultural University, Taian, Shandong 271018, China.

[d]Laboratory of Plant Developmental Biology, Wageningen University, PO Box 8123, 6700 ES Wageningen, the Netherlands.

[1]These authors contributed equally to this work.

[2]Correspondence:

Chuanyou Li	PhD/Professor	Email: cyli@genetics.ac.cn
Qian Chen	PhD/Professor	Email: chenqiangenetics@163.com
Wenkun Zhou	PhD	Email: wenkun.zhou@wur.nl

Keywords:

Mediator, root development, transcription regulation, *SCARECROW*, *SHORTROOT*

www.pnas.org/cgi/doi/10.1073/pnas.1800592115

SUPPLEMENTARY MATERIALS AND METHODS

Plant Material and Growth Conditions.

Arabidopsis thaliana ecotypes Columbia (Col), C24, Landsberg *erecta* (L*er*), and Wassilewskija (Ws) were used as WT. Some of the plant materials used in this study were previously described: *scr-1* (1); *shr-1* (2); *pSCR::GFP:SCR* (3); *pSCR::GFP* (4); *pSHR::SHR:GFP* (5); *pCO2::H2B:YFP* (6); *p35S::SCR:GFP* (7); *pJKD::JKD:YFP* (8). *J0571* was obtained from the Haseloff enhancer trap GFP line collection (http://www.plantsci.cam.ac.uk/Haseloff).

Seeds were surface-sterilized for 12 min in 10% commercial kitchen bleach, washed five times with sterile water, and plated on 1/2MS (9) medium with 1% sucrose and 0.8% agar. Plants were stratified at 4°C for 2 days in the dark and then transferred to a phytotron set at 22°C with a 16 h light/8 h dark photoperiod (light intensity: 120 μmol photons $m^{-2}s^{-1}$) in vertically or horizontally oriented Petri dishes. Roots were examined at 3 to 6 DAG, depending on the experimental requirements.

Plasmid Construction and Plant Transformation.

The promoter region and coding sequence of MED31 were amplified with Gateway-compatible primers (Table S1). The PCR products were cloned by pENTR Directional TOPO cloning kits (Invitrogen). The ENTR clones with the *MED31* promoter region were recombined with the binary vector *pGWB3* (no promoter, GUS) to generate the *pMED31::GUS* construct. The ENTR clones with the *MED31* coding sequence were combined with the binary vector *pGWB5* (35S promoter, GFP) to generate the *p35S::MED31:GFP* (*MED31-GFP*) construct. For the *pMED31::MED31:GFP* construction, the region containing the GFP-coding sequence and NOS-T fragment from the *pGFP-2* vector, the promoter region of *MED31*, and its genomic DNA were sequentially cloned in frame into the binary vector *pCAMBIA1300* using the restriction enzyme cloning method. All the constructs were transformed into *Agrobacterium*

tumefaciens strain GV3101, which was used for transformation of *Arabidopsis* plants by the floral dip method. Transformants were selected based on their resistance to hygromycin. Homozygous T3 or T4 transgenic plants were used for further experiments.

Generation of *med31-c* Using CRISPR/Cas9 Technology.

A 20-base pair (bp) fragment of the *MED31* CDS (65–84 bp) was used as the targeting sequence for genome editing of *MED31*. The designed targeting sequence was cloned into the *Bsa* I site of the *AtU6-26-sgRNA-SK* vector (10). The *AtU6-26-MED31-target-sgRNA* was digested by *Spe* I and *Nhe* I, and the cassette was cloned into the *Spe* I position of the *pYAO:hSpCas9* vector (10) to generate *pYAO:hSpCas9-MED31-target-sgRNA* for *Arabidopsis* transformation. WT Col-0 were transformed with the CRISPR construct by floral dipping. A total of 29 of 35 T1 transformants were successfully edited, which were selected based on their resistance to hygromycin and DNA sequences. The Cas9-free plants with mutations in the T2 progeny were identified for further experiments.

Generation of *MED31-RNAi* Lines.

Two different fragments of the *MED31* CDS were used to generate *MED31-RNAi* lines. Fragment 1 (17–280 bp) and Fragment 2 (273–586 bp) spanned almost the whole *MED31* coding sequence and represented highly specific sequences in the *Arabidopsis* genome. Each fragment was respectively inserted into the *Xho* I and *Bgl* II sites (for the forward insert) and the *Xba* I and *Sal* I sites (for the reverse insert) of the *pUCCRNAi* vector. Then, the *RNAi* constructs were inserted into the *Pst* I site of the *pCAMBIA2300* binary vector behind the 35S promoter. The resulting *p35S::MED31-RNAi* plasmid was transformed into *Agrobacterium tumefaciens* strain GV3101 and used to transform *Arabidopsis* WT Col-0 by the floral dip method. Transformants were selected on the 1/2 MS medium based on their resistance to kanamycin. In total, 78 independent *MED31-RNAi* lines were obtained. Homozygous T3 or T4 lines were selected for

further molecular and phenotypic characterization.

Histology and Microscopy.

Histochemical staining for GUS activity in transgenic plants was performed as described previously (11). Whole seedlings were immersed in the GUS staining solution (1 mM X-glucuronide in 100 mM sodium phosphate, pH 7.2, 0.5 mM ferricyanide, 0.5 mM ferrocyanide, and 0.1% Triton X-100), treated briefly under vacuum, and incubated at 37°C in the dark for 1 h. Differential interference contrast (DIC) images were captured using the Leica DM5000B microscope. Images were processed with Spot Flex software. Modified pseudo-Schiff propidium iodide (mPS-PI) staining was performed according to the protocol described previously (12). For confocal laser scanning microscopy, the root tips of 4 to 6 DAG seedlings were stained in 10 μg/mL PI (Sigma P-4170) for 5 min and observed using a Zeiss LSM 710 system. PI was visualized using wavelengths of 600–640 nm. Wavelengths used to visualize GFP and YFP were 500–540 and 525–565 nm, respectively. Images were taken with ZEN 2012 software (Zeiss). To test 26S-proteasome-dependent protein degradation, 5 DAG *pMED31::MED31:GFP* seedlings were transferred to liquid MS media supplemented 50 μM MG132 for 6 h. The MED31-GFP levels were measured in ZEN software on unmodified root images. For marker expression control, at least 20 seedlings were used for each sample and representative images were shown. The SHR-GFP quantification was performed as previously described (13). The same offset and gain settings were used for both the WT and *MED31-RNAi* seedlings, and SHR-GFP levels were measured in ZEN software on unmodified root images. In all cases, only roots with clear nuclear localized signal in the endodermis were used for calculation. The average pixel intensity in the circled region in the endodermis was calculated using ZEN. In the same longitudinal domain as that of the measured endodermal cell, the average stele intensity was determined (as shown in the boxed region in Fig. 3 *A* and *B*), yielding the endodermal-to-stele ratio. More than six pairs measurements were

made for each root. Twenty roots were used for the analysis, and Fig. 3 *A* and *B* show representative roots.

Y2H Assays.

Y2H assays were based on the MATCHMAKER GAL4 Two-Hybrid System (Clontech). The full-length coding sequences of *SHR* and *SCR* were amplified with the primers listed in Table S1 and cloned into the *pGADT7* vector for the Y2H screening of *pGBKT7-MEDs* constructed with the coding regions of Mediator subunits. To map the domains of MED31 involved in the MED31-SCR interaction, the coding sequences of *MED31* and its derivatives were cloned into the *pGBKT7* vector. To map the domains of SCR involved in the MED31-SCR interaction, the coding sequences of *SCR* and its derivatives were cloned into the *pGADT7* vector, and the full-length coding sequence of *MED31* was cloned into the *pGBKT7* vector. Primers used are listed in Table S1. All the constructs used for testing the interactions were co-transformed into *Saccharomyces cerevisiae* strain AH109. The presence of transgenes was confirmed by growth on SD/-Leu/-Trp (SD/-2) plates. Protein interactions were assessed by dropping the yeast transformants on SD/-Ade/-His/-Leu/-Trp (SD/-4) plates. Interactions were observed after 3 days of incubation at 30°C.

Y3H Assays.

The full-length coding sequence of *SCR* was cloned into the *pGADT7* vector. For the construction of *pBridge-MED31-SHR*, the *MED31* coding region was cloned into the MCS I site of the *pBridge* vector (Clontech) fused to the GAL4 DNA-binding domain, and the coding sequence of *SHR* was cloned into the MCS II site of the *pBridge* vector expressed as the “bridge” protein only in the absence of methionine. Y3H assays were based on the MATCHMAKER GAL4 Two-Hybrid System (Clontech). Constructs used for testing the interactions were co-transformed into *Saccharomyces cerevisiae* strain AH109. The presence of the transgenes was confirmed by growth on SD/-Leu/-Trp

(SD/-2) plates. The transformed yeasts were spread on the plates containing SD/-Ade/-His/-Leu/-Trp (SD/-4) medium to assess the MED31-SCR interaction without the expression of SHR. The plates containing SD/-Ade/-His/-Leu/-Trp/-Met (SD/-5) medium were used to induce SHR expression. Interactions were observed after 3 days of incubation at 30°C. For the construction of *pBridge-SCR-MED31*, the *SCR* coding sequence was cloned into the MCS I site and the *MED31* coding sequence was cloned into the MCS II site of the *pBridge* vector and expressed as the "bridge" protein to test its effects on the SHR-SCR interaction. The experimental procedures were the same as those described above.

LCI Assays.

LCI assays were performed with *N. benthamiana* leaves as previously described (14). The full-length coding sequence of *MED31* was cloned into *pCAMBIA1300-nLUC*, and the full-length coding sequence of *SCR* was cloned into *pCAMBIA1300-cLUC*. Primers used for vector construction are shown in Table S1. The constructs were introduced into *Agrobacterium tumefaciens* strain GV3101. GV3101 carrying the indicated constructs was cultured in Luria-Bertani (LB) medium at 28°C overnight, and then transferred to fresh LB medium with 10 mM 2-(N-morpholine)-ethanesulfonic acid (MES; pH 5.6) and 40 μM acetosyringone (1:100 ratio, v/v) for 16 h. The culture was pelleted and resuspended in 10 mM $MgCl_2$ containing 0.2 mM acetosyringone to a final concentration of OD_{600} = 1.5. Bacteria were kept at room temperature for at least 3 h without shaking. For co-transformation, equal volumes of *Agrobacterium* suspensions carrying the indicated constructs were infiltrated into *N. benthamiana* leaves. After infiltration, plants were incubated at 23°C for 72 h with 16 h light/8 h dark before measuring LUC activity. A low-light cooled CCD imaging apparatus (NightOWL II LB983 with indigo software) was used to capture the LUC image. Leaves were sprayed with 0.5 mM luciferin and placed in the dark for 3 min before luminescence detection.

Antibody Preparation.

The coding region of *MED31* was amplified from WT cDNA using gene-specific primers (Table S1). The PCR product was cloned into the *pMAL-c2X* vector to express the MED31-MBP fusion in *E. coli* BL21 (DE3). The recombinant proteins were used to raise polyclonal antibodies in mice.

RNA Extraction, Reverse Transcription (RT), and RT-Quantitative PCR (RT-qPCR) Assays.

For reverse-transcription quantitative PCR (RT-qPCR) analysis of *MED31* in *MED31-RNAi* lines, total RNA was extracted from 6 DAG seedlings using the Trizol reagent (Invitrogen). For RT-qPCR analysis of *SHR*, *SCR*, and their target genes, approximately 5 mm root tips were harvested from 5 DAG seedlings for RNA extraction. cDNA was prepared from 2 μg of total RNA with Superscript III reverse transcriptase (Invitrogen) and quantified on a Roche 480 cycler with the SYBR Green kit (Takara). The expression levels of target genes were normalized against *ACT7*. Statistical significance was evaluated with the Student's *t* test. Primers are listed in Table S1.

Western Blot Analysis.

Protein extraction and western blotting were performed according to standard protocols. Seedlings were ground into fine powders in liquid nitrogen and then transferred to extraction buffer (50 mM Tris-HCl, pH 7.5, 150 mM NaCl, 10 mM EDTA, 50 mM DTT, 2% [v/v] Nonidet P-40, and protease inhibitor cocktail [Roche]). For western blot analysis, protein samples were boiled for 5 min after mixing with sodium dodecyl sulfate (SDS) loading buffer, separated by SDS-polyacrylamide gel electrophoresis, and transferred to polyvinylidene fluoride membranes. Immunoblots were probed with an anti-MED31 antibody (1:2,000). Ponceau S-stained membranes were used as loading controls.

Co-IP Assays.

Co-IP assays in *Arabidopsis thaliana* were performed according to a published procedure (15) with minor modifications. In brief, 6 DAG *p35S::SCR:GFP* and WT Col-0 seedlings were homogenized in protein lysis buffer respectively (50 mM Tris-HCl, pH 7.5, 150 mM NaCl, 5 mM EDTA, 0.1% Triton X-100, 0.2% Nonidet P-40, 0.6 mM PMSF, and 20 μM MG132 with Roche protease inhibitor cocktail). After protein extraction, 20 μL of protein A/G plus agarose beads (Santa Cruz Biotechnology) was added to the 2 mg extracts to reduce nonspecific immunoglobulin binding. After 1 h of incubation, the supernatant was transferred to a new tube. GFP antibody-bound agarose beads (MBL) were then added to each reaction for 4 h at 4°C. Col-0 seedlings were used as negative controls. The precipitated samples were washed at least four times with the lysis buffer and then eluted by boiling the beads in SDS protein loading buffer for 5 min. Immunoblots were detected with anti-MED31 antibody (1:2,000) and anti-GFP antibody (Abmart, 1:2,000).

Co-IP assays using *N. benthamiana* leaves were performed according to a published procedure (16). *Agrobacterium tumefaciens* strain GV3101 carrying *p35S::SCR:GFP* or *p35S::MED31:myc* constructs was co-infiltrated into tobacco leaves. The co-transformed tobacco leaves were ground to a fine powder and transferred to lysis buffer (50 mM Tris-MES, pH 8.0, 0.5 M sucrose, 1 mM $MgCl_2$, 10 mM EDTA, 5 mM DTT, 0.5 mM PMSF, and 50 μM MG132 with Roche protease inhibitor cocktail). After protein extraction, the sequential procedures were the same as those used for Co-IP assays in *Arabidopsis*. Co-IP assays for testing the association of SHR, SCR, and MED31 using *N. benthamiana* leaves were similar except that the extracts contained three co-transformation proteins.

Co-IP assays in *N. benthamiana* were also used to confirm the competition between SHR and MED31 for interaction with SCR. *p35S::SCR* and *p35S::MED31:myc* were co-infiltrated into tobacco leaves, whereas *p35S::SHR:GFP* was separately transformed. Proteins were extracted using the lysis buffer described

above. For each reaction, the SCR and MED31-myc protein extracts were equal. SHR-GFP protein extracts were added to SCR and MED31-myc protein extracts according to the concentration gradient. The mixed protein extracts were manipulated as described for the Co-IP assays in *Arabidopsis*. For another set of assays, SCR and SHR-GFP proteins were co-expressed and extracted, whereas MED31-myc was separately expressed, and added in a gradient. Immunoblots were probed with the following antibodies: anti-GFP (Abmart, 1:2,000); anti-myc (Abmart, 1:2,000); and anti-SCR (Santa Cruz, 1:200).

In vitro quantitative Co-IP assays were used to confirm the different affinity of SCR for SHR or MED31. The full-length coding sequence of *SCR* with a C-terminal FLAG tag was cloned into the pF3KWG (BYDV) Flexi Vector (Promega). Then, SCR-FLAG was synthesized by *in vitro* transcription/translation reactions (Promega). The full-length coding sequences of *SHR* and *MED31* were cloned into the *pMAL-c2X* vector. Primers are listed in Table S1. SHR-MBP and MED31-MBP were expressed in *E. coli* BL21 (DE3) and purified using an amylose resin (NEB). 10 μL of the SCR-FLAG reaction product and 1 μg of SHR-MBP proteins were used in each reaction, and MED31-MBP was added according to the concentration gradient ratio of SHR-MBP. M2 Gel (10 μL) (anti-FLAG, Sigma) was added to 1 mL of reaction buffer (25 mM Tris-HCl, pH 7.5, 100 mM NaCl, 1 mM DTT, and Roche protease inhibitor cocktail) with protein samples and incubated at 4°C for 1 h. The beads were collected and washed with washing buffer (25 mM Tris-HCl, pH 7.5, 150 mM NaCl, and 1 mM DTT) three times. The bound proteins were eluted with elution buffer (25 mM Tris-HCl, pH 7.5, 100 mM NaCl, 1 mM DTT, and 300 μg/mL 3× FLAG). SHR-MBP and MED31-MBP were detected by western blotting using an anti-MBP antibody (NEB, 1:20,000), and signals were quantified using Image J software.

***In Vitro* Pull-Down Assays.**

For the pull-down assays to detect the MED31-SCR or SHR-MED31 interactions,

SHR-FLAG and SCR-FLAG proteins were synthesized by *in vitro* transcription/translation reactions (Promega). The MED31-MBP protein was affinity purified. For each reaction, 15 μL of agarose beads bound with 1 μg of MED31-MBP was incubated with 10 μL of SHR-FLAG or SCR-FLAG synthesized product in 1 mL of reaction buffer (25 mM Tris-HCl, pH 7.5, 100 mM NaCl, 1 mM DTT, and Roche protease inhibitor cocktail) at 4°C for 1 h. Then, the beads were collected and washed three times with washing buffer (25 mM Tris-HCl, pH 7.5, 150 mM NaCl, and 1 mM DTT). The bound proteins were eluted using elution buffer (25 mM Tris-HCl, pH 7.5, 100 mM NaCl, 1 mM DTT, and 10 mM maltose). SHR-FLAG and SCR-FLAG were detected by western blotting using an anti-FLAG antibody (Abmart, 1:2,000). The purified MBP was used as the negative control. For pull-down assays to test the SHR-SCR and SHR-SHR interactions, the full-length coding sequence of *SHR* was PCR-amplified and cloned into the *pGEX-4T-3* vector. The GST-SHR protein was expressed in *E. coli* BL21 (DE3) and affinity purified using GST Bind Resin (Millipore). The sequential procedures were the same as those described above. For pull-down assays to test the SHR-SCR and SCR-SCR interactions, the GST-SCR protein was synthesized by *in vitro* transcription/translation reactions (Promega). The sequential manipulation was similar to the experimental procedures described above.

Pull-down assays to confirm that MED31 forms a ternary complex with SCR and SHR were performed with 1 μg of purified MED31-MBP, GST-SHR, and 10 μL of SCR-FLAG synthesized product. The amylose resin (NEB) was used to pull down proteins. Samples with purified MBP proteins or without SCR-FLAG product were used as negative controls. The sequential procedures and buffers were the same as those described above.

For pull-down assays to confirm that a high concentration of MED31 affects the SHR-SCR interaction, 1 μg of purified GST-SHR and 10 μL of SCR-FLAG synthesized product were added to each sample. Purified MED31-MBP was added according to the concentration gradient. The amylose resin (NEB) and GST Bind Resin (Millipore) were

used to pull down proteins. The sequential procedures and buffers were the same as those described above.

ChIP-qPCR Assays.

Root tips of WT, *pSCR::GFP:SCR*, and *pMED31::MED31:GFP* at 5 DAG, and 5 DAG seedlings of *MED31-GFP/WT* and *MED31-GFP/scr-1*, and 5 DAG seedlings of *WT* and *MED31 RNAi* were harvested respectively and cross-linked with 1% formaldehyde at room temperature for 10 min, followed by neutralization with 0.125 M glycine. The chromatin complex was isolated, resuspended in lysis buffer (50 mM HEPES [pH 7.5], 150 mM NaCl, 1 mM EDTA, 1% SDS, 1% Triton X-100, 0.1% sodium deoxycholate, and 1 mM PMSF, with 1× Roche protease inhibitor cocktail), and sheared by sonication to reduce the average DNA fragment size to around 200 bp. The sheared chromatin was pre-cleared with Protein A salmon sperm-coupled agarose (Millipore), and 10 μL of the pre-cleared chromatin was removed for use as an input control. The chromatin complex was immunoprecipitated overnight at 4°C with anti-GFP (Abcam, ab290) or anti-Pol II CTD antibodies. The immunoprecipitated chromatin complex was washed with low-salt buffer (20 mM Tris-HCl [pH 8.0], 2 mM EDTA, 150 mM NaCl, 0.5% Triton X-100, and 0.2% SDS), high-salt buffer (20 mM Tris-HCl [pH 8.0], 2 mM EDTA, 500 mM NaCl, 0.5% Triton X-100, and 0.2% SDS), LiCl buffer (10 mM Tris-HCl [pH 8.0], 1 mM EDTA, 0.25 M LiCl, 0.5% NP-40, and 0.5% sodium deoxycholate), and TE buffer (10 mM Tris-HCl [pH 8.0] and 1 mM EDTA). After washing, the immunoprecipitated chromatin was eluted with elution buffer (1% SDS and 0.1 M $NaHCO_3$). Protein-DNA cross-linking was reversed by incubating the immunoprecipitated complexes at 65°C overnight. DNA was recovered using the QIAquick PCR purification kit (Qiagen). The ChIP signal was quantified as the percentage of total input DNA by qPCR at the loci of *CYCD6;1* and other SCR target genes and normalized to *ACT7* in the WT or *MED31-GFP*. Primers used for qPCR are listed in Table S1.

SUPPLEMENTARY FIGURES

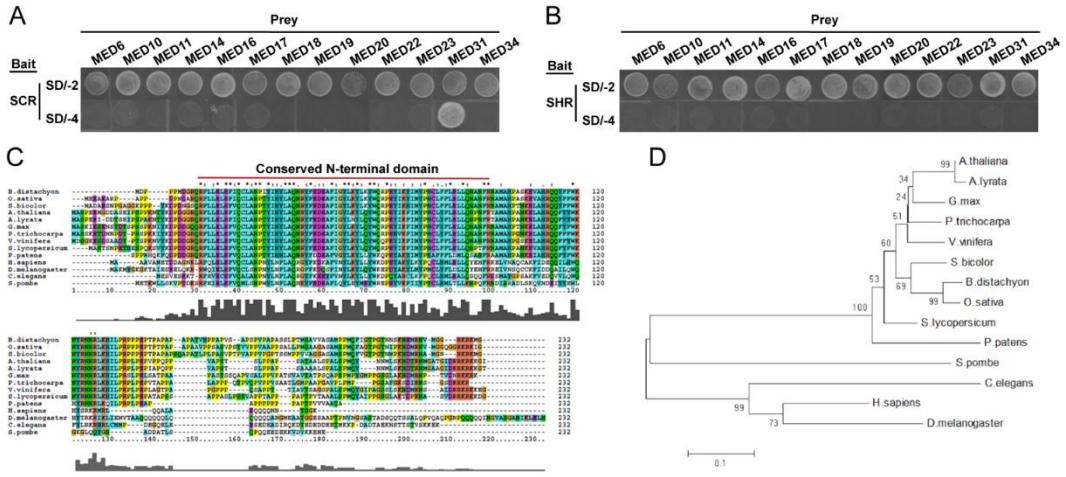

Fig. S1. The highly conserved *Arabidopsis* Mediator subunit MED31 interacts with SCR but not SHR. (*A and B*) Y2H assays were used to screen the interactions of SCR-MEDs and SHR-MEDs. Yeast cells co-transformed with pGADT7-SCR or pGADT7-SHR (prey) and pGBKT7-MEDs (bait) were dropped onto SD/-Trp/-Leu (SD/-2) and SD/-Ade/-His/-Trp/-Leu (SD/-4) medium to assess protein-protein interactions. MEDs, Mediator subunits. (*C*) Alignment of MED31 proteins among different species using the ClustalX2 software. Identical amino acids are indicated in the same color. The red line represents the conserved N-terminal domain. (*D*) Phylogenetic analysis of MED31 and its orthologs from yeast to humans.

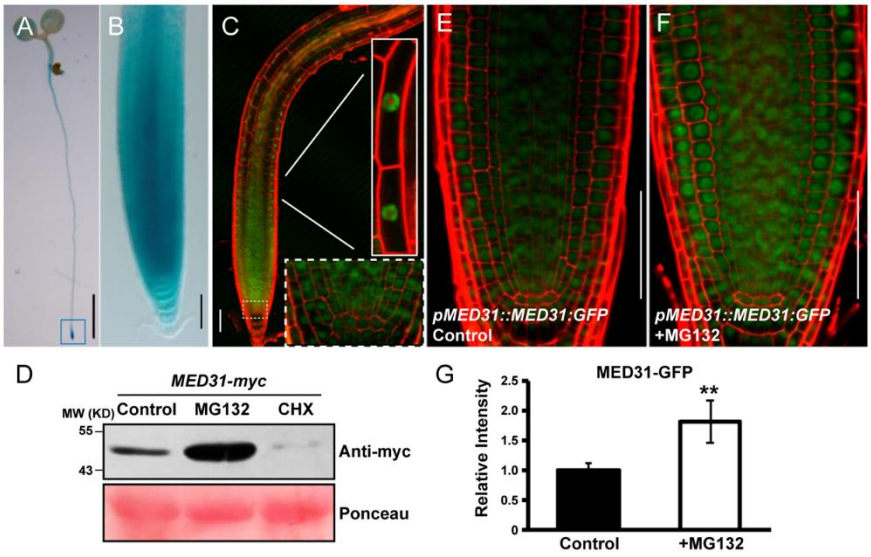

Fig. S2. Expression pattern and subcellular localization of MED31.(*A* and *B*) *pMED31::GUS* expression pattern in whole seedlings (*A*) and RAM (*B*). Scale bars, 2 mm in (*A*), 50 μm in (*B*). (*C*) *pMED31::MED31:GFP* expression pattern in the root meristem and the subcellular localization of the MED31 protein. The inset surrounded by the white rectangle shows the localization of MED31 to the nucleus. The inset surrounded by the white dashed rectangle shows the root stem cell niche. Scale bar, 50 μm. (*D*) The 6 DAG seedlings of *MED31-myc* were treated with 50 μM MG132 or 100 μM cycloheximide (CHX) for 6 h before total proteins were extracted for western blotting using an anti-myc antibody. Ponceau S-stained membranes are shown as the loading control. (*E* and *F*) Expression patterns prior to and after MG132 treatment for 5 DAG *pMED31::MED31:GFP* seedlings. Scale bars, 50 μM . (*G*) Quantification of *pMED31::MED31:GFP* GFP fluorescence intensity in the root meristem as shown in (*E*) and (*F*). Data shown are average and SD (n = 20). (Student's *t* test, $^{**}P < 0.01$).

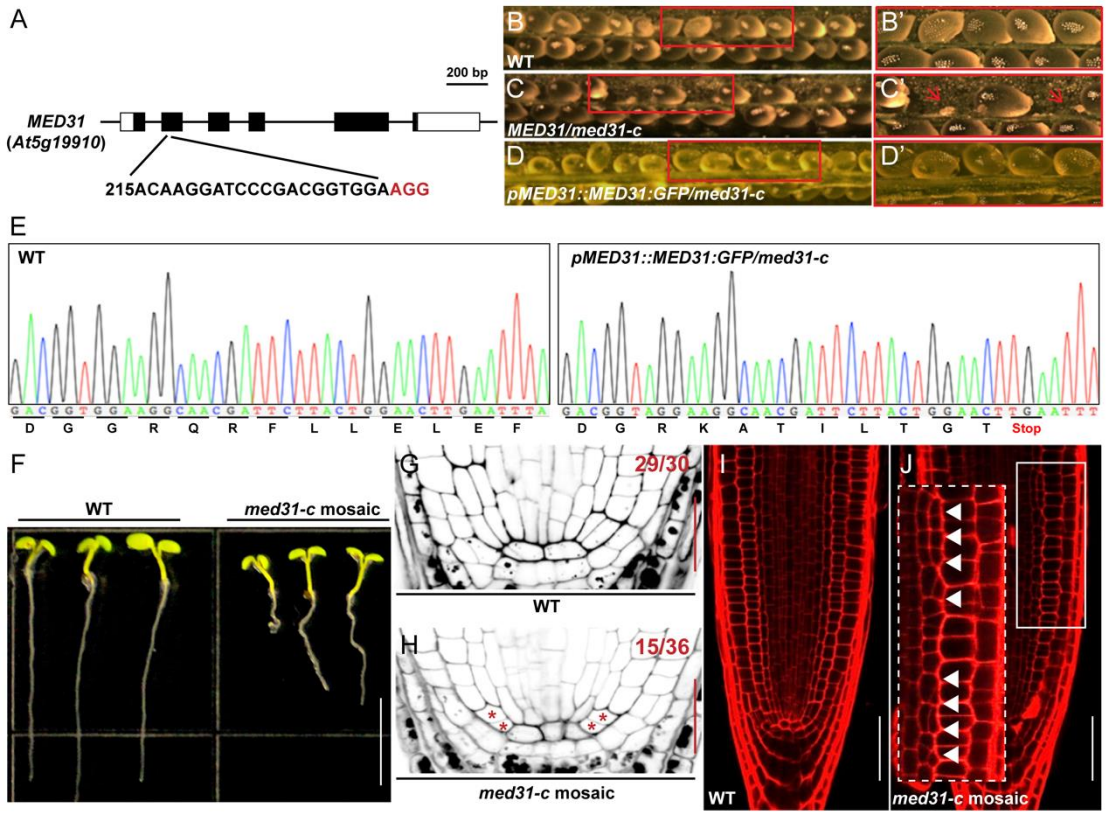

Fig. S3. Construction and characterization of *med31-c* plants. (*A*) Schematic diagram of *MED31*. The fragment was used for the target sequence of CRISPR/Cas9. (*B-D′*) The open siliques of WT (*B*), *MED31/med31-c* (*C*), and *pMED31::MED31:GFP med31-c* (*D*) plants. (*B*) Green seeds in the silique of WT plants. (*C*) Lethal seeds among green seeds in the silique of *MED31/med31-c* plants. (*D*) Green seeds in the silique of *pMED31::MED31:GFP/med31-c*. (*B′-D′*) Magnifications of the images in the red rectangles in (*B-D*). The red arrows indicate lethal seeds in the silique of *MED31/med31-c*. (*E*) DNA sequencing peak in the WT and *pMED31::MED31:GFP med31-c*. The peaks indicated by red rectangles are the insertion sites. (*F*) Phenotypes of WT and *med31-c* mosaic seedlings at 5 DAG. Scale bar, 5 mm. (*G* and *H*) Delayed ACD in CEI/CEID of *med31-c* mosaic. mPS-PI staining of WT (*G*) and *med31-c* mosaic (*H*) root tips at 3 DAG. Red asteriskss mark the undivided CEI and CEID cells in *med31-c* mosaic. Scale bars, 20 μm. (*I* and *J*) PI staining of WT (*I*) and *med31-c* mosaic (*J*) root tips at 6 DAG. The inset shows root radial patterning surrounded by white rectangles in (*J*). Arrowheads indicate abnormally periclinal cell divisions in *med31-c* mosaic. Scale bars, 50 μm.

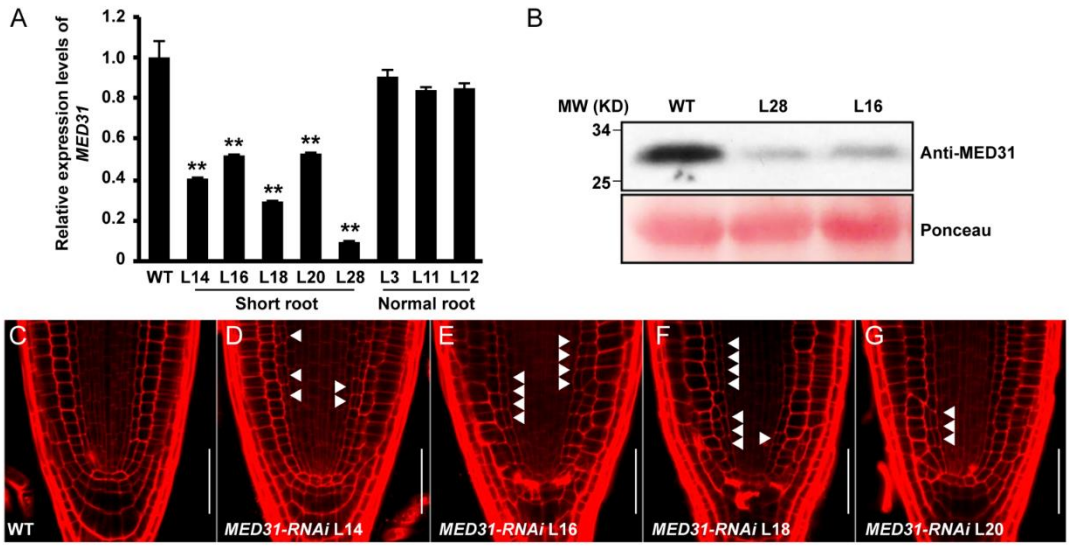

Fig. S4. Construction of *MED31-RNAi*.(*A*) Relative expression levels of *MED31* mRNA measured by RT-qPCR in *p35S::MED31-RNAi* transgenic lines. L, line. (*B*) Protein gel analyses showing the significantly reduced levels of MED31 in *p35S:MED3-RNAi* lines using anti-MED31 antibodies. Ponceau S-stained membranes are shown as loading controls. (*C*-*G*) PI staining of WT (*C*) and *MED31-RNAi* lines (*D*-*G*) root tips at 5 DAG. Arrowheads indicate abnormally periclinal cell divisions in *MED31-RNAi* lines. Scale bars, 50 μm.

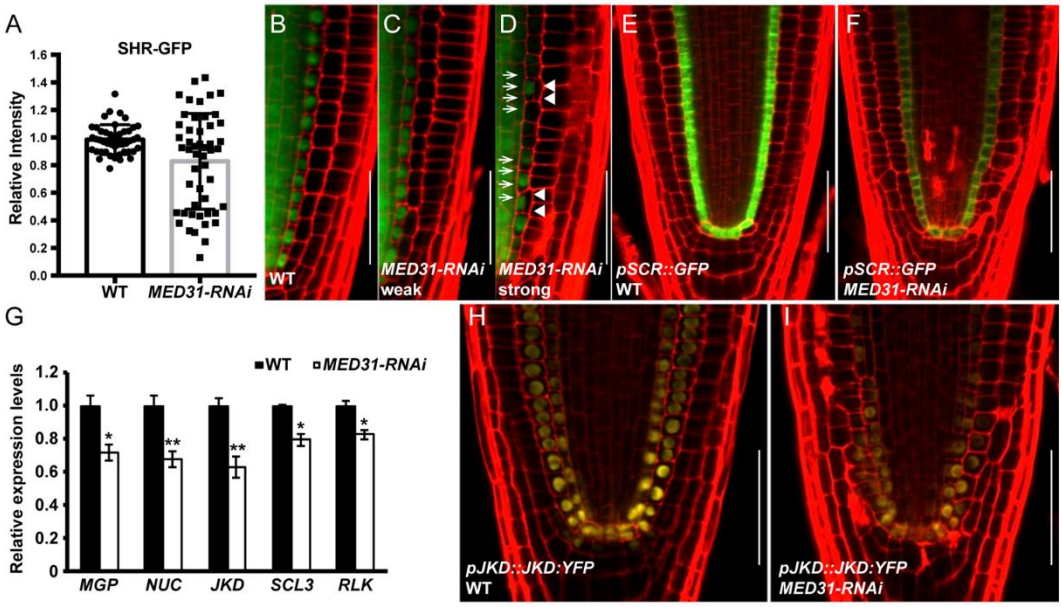

Fig. S5. Reduction of *MED31* impairs the expression of SCR and its targets. (*A*) Quantification of the endodermal-to-stele ratios of SHR-GFP fluorescence. Data shown are average and SD (n = 50). Each dot denotes an endodermal-to stele ratio of SHR-GFP fluorescence. (*B-D*) *pSHR::SHR:GFP* expression in WT (*B*), weak phenotypes (*C*) and strong phenotypes (*D*) of *MED31-RNAi*. Arrows in (D) show variations of SHR-GFP pattern in endodermal cells. Scale bars, 50 μm. (*E* and *F*) *pSCR::GFP* expression in the WT (*E*) and *MED31-RNAi* (*F*) at 6 DAG. Scale bars, 50 μm. (*G*) qPCR analysis showing the relative expression levels of SCR targets in the WT and *MED31-RNAi*. Total RNA was extracted from 0.5 cm root tip sections of 5 DAG seedlings. Error bars represent SD from three independent experiments (Student's *t* test, $*P < 0.05$, $**P < 0.01$). (*H* and *I*) *pJKD::JKD:YFP* expression in the WT (H) and *MED31-RNAi* (I) at 6 DAG. Scale bars, 50 μm.

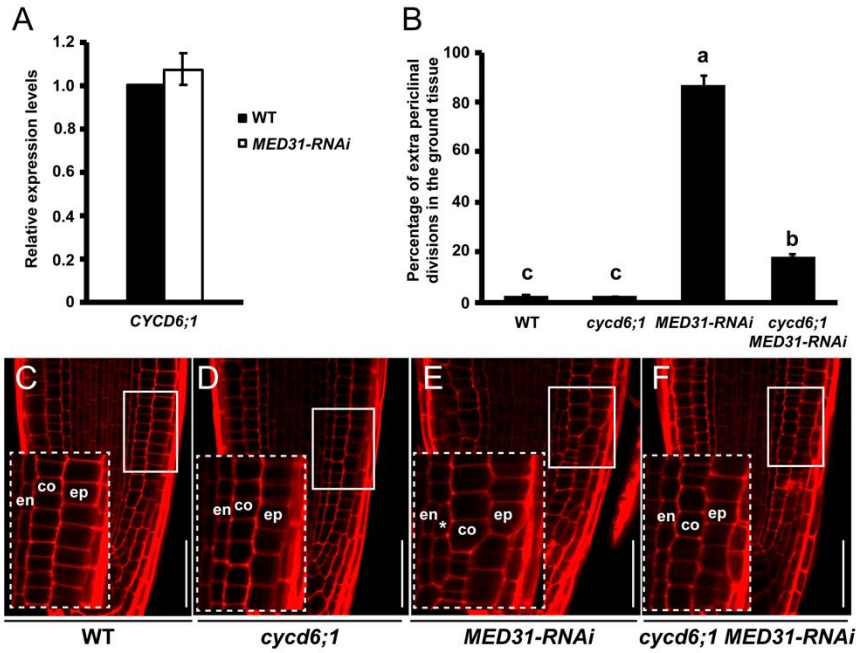

Fig. S6. The ground tissue patterning defects of *MED31-RNAi* were partially rescued by *cycd6;1*. (*A*) qPCR analysis showing the relative expression levels of *CYCD6;1* in the WT and *MED31-RNAi*. Total RNA was extracted from 5 DAG seedlings. Error bars represent SD from free three independent experiments. (*B*) Extra periclinal divisions rate in the ground tissue of WT, *cycd6;1*, *MED31-RNAi*, *cycd6;1 MED31-RNAi*. Data shown are average and SD (n = 40). Samples with different letters are significantly different at $P < 0.01$. (*C-F*) Root apical meristem phenotypes of WT (*C*), *cycd6;1* (*D*), *MED31-RNAi* (*E*), and *cycd6;1 MED31-RNAi* (*F*) seedlings at 5 DAG. The insets show the root radial patterning surrounded by the white rectangle. En, endodermis; co, cortex; ep, epidermis; *, irregular cell divisions in *MED31-RNAi*. Scale bars, 50 μm.

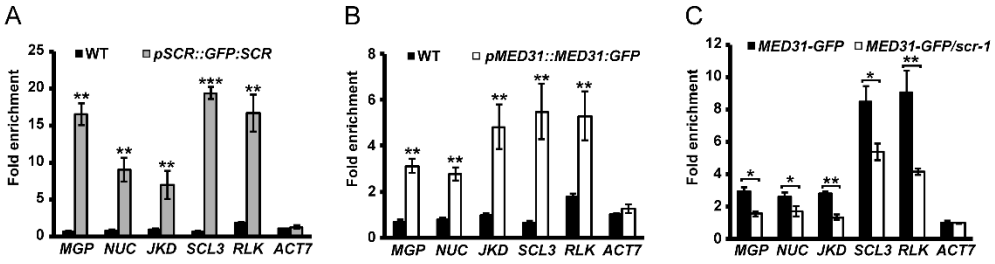

Fig. S7. MED31 is recruited to SCR target promoters in a SCR-dependent manner. (*A* and *B*) ChIP-qPCR results showing the enrichment of SCR (*A*) and MED31 (*B*) on the promoter regions of other SCR targets. Sonicated chromatins from 5 DAG WT, *pSCR::GFP:SCR*, and *pMED31::MED31:GFP* seedlings were precipitated with an anti-GFP antibody (Abcam), respectively. The precipitated DNA was used as template for qPCR analysis with primers targeting the promoter regions of SCR targets. The ChIP signal was quantified as the percentage of the total input DNA and normalized to *ACT7* in the indicated genotypes, respectively. (*C*) ChIP-qPCR results showing that the *scr* mutation impairs the recruitment of MED31 to the promoter regions of other SCR targets. Chromatins were extracted from *MED31-GFP* and *MED31-GFP/scr-1* seedlings at 5 DAG and precipitated with anti-GFP antibodies (Abcam), respectively. The ChIP signal was quantified as the percentage of total input DNA by qPCR and set to *ACT7* in the indicated genotypes, respectively. *ACT7* was used as a nonspecific binding site. Error bars represent SD from three independent experiments. Asterisks indicate significant differences according to the Student's *t* test, **P* < 0.05, ***P* < 0.01, ****P* < 0.001.

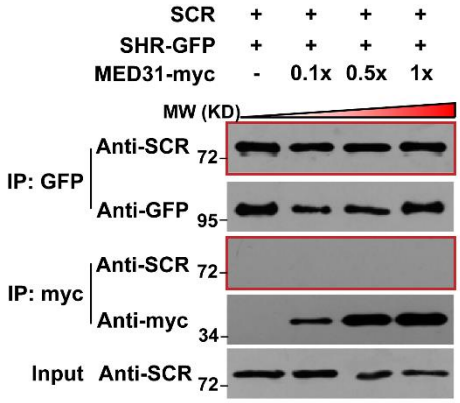

Fig. S8. Low concentrations of MED31 show minor effect on the SHR-SCR interaction revealed by Co-IP assays. SCR and SHR-GFP were co-expressed in *N. benthamiana* leaves. MED31-myc was added to SCR and SHR-GFP protein extracts according to the indicated gradient. Protein samples were immunoprecipitated with anti-GFP antibodies or anti-myc antibodies and immunoblotted with anti-SCR antibodies to detect the SHR-SCR interaction and the MED31-SCR interaction, respectively.

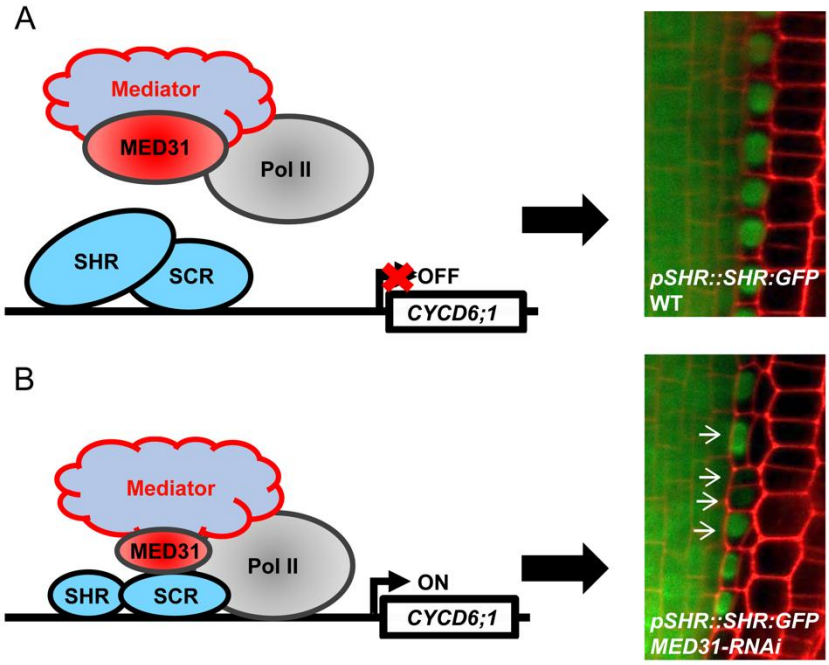

Fig. S9. Proposed model by which MED31 regulates SHR-SCR-mediated patterning of upper ground tissue. In the endodermal layer of WT roots, the relative protein abundance of SHR and MED31 in individual cells is uniformly maintained at "high levels" sufficient to prevent the MED31-SCR interaction; *CYCD6;1* expression is turned off (*A*). In the presumptive endodermal layer of *MED31-RNAi* roots, the protein abundance ratio of SHR to MED31 is impaired, thereby leading to sporadic activation of *CYCD6;1* expression, which coincides with irregular periclinal divisions in upper ground tissue (*B*).

SUPPLEMENTARY TABLES

Table S1 Primers used in this study

Primer Name	Primer Sequence (5'-3')	Use
SCR-EcoRI-FP	AAAGAATTCATGGCGGAATCCGGCGAT	Y2H
SCR-BamHI-RP	AAAGGATCCCTAAGAACGAGGCGTCCA	
SCR-795-BamHI-RP	AAAGGATCCTGTTTGGACGGCGGGAAC	
SCR-796-EcoRI-FP	AAAGAATTCAATACGGCGGAGGCTTTA	
SCR-1458-BamHI-RP	AAAGGATCCCACAGCTTCCCTTTTCCT	
SCR-1459-EcoRI-FP	AAAGAATTCGCTGTTCACTGGCTTCAA	
SHR-EcoRI-FP	AAAGAATTCATGGATACTCTCTTTAGA	
SHR-BamHI-RP	AAAGGATCCTTACGTTGGCCGCCACG	
MED31-EcoRI-FP	AAAGAATTCATGGCTTCGCCAGAGGAGAT	
MED31-XhoI-RP	TTTCTCGAGTATACCCTTCTTTCTCTTCCTACGATCA	
MED31-SalI-RP	TTTGTCGACTATACCCTTCTTTCTCTTCCTACGATCA	pMAL
MED31-393-XhoI-RP	TTTCTCGAGTAGAATGTGCTTCAGTCTGTTG	
MED31-393-SalI-RP	TTTGTCGACTAGAATGTGCTTCAGTCTGTTG	
MED31-394-EcoRI-FP	AAAGAATTCCCTCGGCCTCTTCCAGAGCC	
SHR-SgfI-FP	TCCGCGATCGCATGGATACTCTCTTTAGACTA	
SHR-FLAG-PmeI-RP	TCCGTTTAAACCTTGTCATCGTCATCCTTGTAGTCCGTTGG CCGCCACGCACTAGC	
SCR-SgfI-FP	TCCGCGATCGCATGGCGGAATCCGGCGATTTC	
SCR-FLAG-PmeI-RP	TCCGTTTAAACCTTGTCATCGTCATCCTTGTAGTCAGAAC GAGGCGTCCAAGCTGA	
SCR-KpnI-FP	CGGGGTACCATGGCGGAATCCGGCGATTTC	
SCR-SalI-RP	CGCGTCGACCTAAGAACGAGGCGTCCAAGC	
MED31-KpnI-FP	CGGGGTACCATGGCTTCGCCAGAGGAGATG	
MED31-CDS-FP(cacc)	CACCATGGCTTCGCCAGAGGAGAT	MED31-TOPO
MED31-CDS-RP	TATACCCTTCTTTCTCTTCCTACGATCA	
MED31-273-FR-XhoI-FP	AAACTCGAGACTTCTTCAAAACCCCAACTTCA	*35S:MED31-RNAi*

Primer name	Primer sequence (5'-3')	Use
MED31-586-FR-XbaI-RP	TTTAGATCTTACCCTTCTTTCTCTTCCTACGAT	
MED31-17-F2R2-XhoI-FP	AAACTCGAGAGATGGGTGATGATGCATC	
MED31-280-F2R2-XbaI-RP	TTTAGATCTGAAGAAGTTCAAGGAAATATAG	
MED31-65-84-BsaI-FP	ATTGACAAGGATCCCGACGGTGGA	MED31 CRISPR
MED31-65-84-BsaI-RP	AAACTCCACCGTCGGGATCCTTGT	
pMED31-FP(cacc)	CACCCATATATCTGAATGAAGCTGGA	pMED31-TOPO
pMED31-RP	GAACGAACGGAACCTGAAGCAAATTT	
pMED31-SalI-FP	ACGCGTCGACATCTGCCATTCTCCTGGATGA	*pMED31:MED31-GFP*
MED31-Genomic-XbaI-RP	TGCTCTAGATATACCCTTCCTGACATTATATG	
SHR-CDS-FP(cacc)	CACCATGGATACTCTCTTTAGACTAGTCA	SHR-TOPO
SHR-CDS-RP	CGTTGGCCGCCACGCACTAGCC	
SCR-CDS-FP(cacc)	CACCATGGCGGAATCCGGCGAT	SCR-TOPO
SCR-CDS-RP	AGAACGAGGCGTCCAAGCTGAAG	
SHR-BamHI-FP	CGCGGATCCATGGATACTCTCTTTAGACTA	GST-SHR
SHR-EcoRI-RP	CCGGAATTCTTACGTTGGCCGCCACGCACT	
GST-SgfI-FP	TCCGCGATCGCATGTCCCCTATACTAGGTTAT	GST-SCR
SCR-Pme-RP	TCCGTTTAAACCTAAGAACGAGGCGTCCAAGC	
SHR-NotI-FP	ATAAGAATGCGGCCGCAATGGATACTCTCTTTAGACTA	Y3H
SHR-BglII-RP	GGAAGATCTTTACGTTGGCCGCCACGCACT	
MED31-NotI-FP	ATAAGAATGCGGCCGCAATGGCTTCGCCAGAGGAGATG	
MED31-BglII-RP	GGAAGATCTTTATATACCCTTCTTTCTCTT	
scr-1-FP	CCTTCACGGTGGATGCCTCAA	Genotyping
scr-1-RP	CCACAGCTTCCCTTTTCCTCACA	
shr-1-FP	ATGAGTTCTTGAGAGGGTTTGG	
shr-1-RP	TCATCCTCCTCGACCACTTCC	
CaMV-35S-FP	TTCCATTGCCCAGCTATCTGTCAC	*MED31-RNAi*
pUCCRNAi-intron-RP	TTTATCTGGTTTTGAGTGACACA	
cycd6;1-FP	AATTCGACGACCCATCTCTG	

Primer name	Primer sequence (5'-3')	Use
cycd6;1-RP	CTGCAATCACCGATGGTTTA	
GABI-LB	ATATTGACCATCATACTCATTGC	
MED31-q-FP	AAGGAATTGGCGCATAGACA	qPCR
MED31-q-RP	CATTGGAGAAAGGGCTGGAGAG	
SHR-q-FP	TCCAAGGACGAGCAACGAGAGGT	
SHR-q-RP	CCGGCGGCATCAGGACACT	
SCR-q-FP	TTCCCGCCGTCCAAACAAATA	
SCR-q-RP	TGCGCTGAGGTCCCGTAAGG	
MGP-q-FP	CGCTAACGGGGCAACTTCTCTTTC	
MGP-q-RP	GTCGCTGCCACCATCTTCTACAAT	
JKD-q-FP	GCCGTGGCCACAACCTTCC	
JKD-q-RP	TTTCGCATGTGCCTTCCAATCA	
NUC-q-FP	CGGAAACACGGGGAGAAGAA	
NUC-q-RP	TCCGCTAAGGCATCGCAGAAA	
SCL3-q-FP	CTCGCTTCTTCATCTCCGTTTCAT	
SCL3-q-RP	GCATCGTGTCGCCGTCAGG	
RLK-q-FP	GCTCGCGGGCTAACATACG	
RLK-q-RP	GGACTCGGCCCAAACTCAAG	
Actin7-q-FP	CCATTCAGGCCGTTCTTTC	
Actin7-q-RP	CGTTCTGCGGTAGTGGTGA	
CYCD6;1-A-FP	GGGTTTCCTATTTCCAATTTAGGGT	ChIP-PCR
CYCD6;1-A-RP	CAAATGCCAGATTTTGAACCACTTT	
CYCD6;1-B-FP	CAGTCAGGCTTTGGCAGTA	
CYCD6;1-B-RP	AGCTTGGTTTTCCTTGTCC	
CYCD6;1-C-FP	GAGCTCAAAGAAGAAGATCCT	
CYCD6;1-C-RP	AACTGTAGAGGACAGAGCTCG	
pMGP-FP	CTCCGATACATATGCTCAGTCT	
pMGP-RP	ATGCTCCCTATTCGTCTTTT	

Primer name	Primer sequence (5'-3')	Use
pNUC-FP	CTCAGGGATTATTAGTAGTT	
pNUC-RP	TAAGGAGGTATCAAGGTGTG	
pSCL3-FP	TTTTGGGAGTGAGAGGGTTC	
pSCL3-RP	AGATGGATGGGATTGGAAAA	
pRLK-FP	GCGTAATCTCACGTCACAATTTCCG	
pRLK-RP	TGCTGACGTCGCTTTGTCGTTT	
pJKD-FP	CGTAAATCCGTAAAAAGTG	
pJKD-RP	TAAGTTGGGAGAAGGTAT	

SUPPLEMENTARY REFERENCES

1. Di Laurenzio L*, et al.* (1996) The *SCARECROW* gene regulates an asymmetric cell division that is essential for generating the radial organization of the Arabidopsis root. *Cell* 86:423-433.
2. Benfey PN*, et al.* (1993) Root development in *Arabidopsis*: four mutants with dramatically altered root morphogenesis. *Development* 119:57-70.
3. Sabatini S*, et al.* (1999) An auxin-dependent distal organizer of pattern and polarity in the *Arabidopsis* root. *Cell* 99:463-472.
4. Gallagher KL, Paquette AJ, Nakajima K, Benfey PN (2004) Mechanisms regulating SHORT-ROOT intercellular movement. *Curr Biol* 14:1847-1851.
5. Nakajima K, Sena G, Nawy T, Benfey PN (2001) Intercellular movement of the putative transcription factor SHR in root patterning. *Nature* 413:307-311.
6. Heidstra R, Welch D, Scheres B (2004) Mosaic analyses using marked activation and deletion clones dissect *Arabidopsis* SCARECROW action in asymmetric cell division. *Genes Dev* 18:1964-1969.
7. Cruz-Ramírez A*, et al.* (2012) A bistable circuit involving SCARECROW-RETINOBLASTOMA integrates cues to inform asymmetric stem cell division. *Cell* 150:1002-1015.
8. Long Y*, et al.* (2015) Arabidopsis BIRD zinc finger proteins jointly stabilize tissue boundaries by confining the cell fate regulator SHORT-ROOT and contributing to fate specification. *Plant Cell* 27:1185-1199.
9. Murashige T, Skoog F (1962) A revised medium for rapid growth and bio assays with tobacco tissue cultures. *Physiol Plantarum* 15:473-497.
10. Yan L*, et al.* (2015) High-efficiency genome editing in *Arabidopsis* using *YAO* promoter-driven CRISPR/Cas9 system. *Mol Plant* 8:1820-1823.
11. Zhou W*, et al.* (2010) *Arabidopsis* Tyrosylprotein sulfotransferase acts in the

auxin/PLETHORA pathway in regulating postembryonic maintenance of the root stem cell niche. *Plant Cell* 22:3692-3709.

12. Truernit E*, et al.* (2008) High-resolution whole-mount imaging of three-dimensional tissue organization and gene expression enables the study of phloem development and structure in *Arabidopsis*. *Plant Cell* 20:1494-1503.
13. Koizumi K, Hayashi T, Wu S, Gallagher KL (2012) The SHORT-ROOT protein acts as a mobile, dose-dependent signal in patterning the ground tissue. *Proc Natl Acad Sci USA* 109:13010-13015.
14. Chen H*, et al.* (2008) Firefly luciferase complementation imaging assay for protein-protein interactions in plants. *Plant Physiol* 146:368-376.
15. Spoel SH*, et al.* (2009) Proteasome-mediated turnover of the transcription coactivator NPR1 plays dual roles in regulating plant immunity. *Cell* 137:860-872.
16. Liu LJ*, et al.* (2010) An efficient system to detect protein ubiquitination by agroinfiltration in *Nicotiana benthamiana*. *Plant J* 61:893-903.